

N64 13404\*

code/

(NASA CR-5303 0)

Technical Report No. 32-226  
Revision No. 1

**Optimum Interplanetary Rendezvous Trajectories  
with Power-Limited Vehicles**

W. G. Melbourne *and*

C. G. Sauer, Jr.

☒ OTS

☒ 2

(NASA Contract NAS7-100)

JPL-TR-32-226 (Rev. 1)

OTS: PRICE

XEROX

\$

2.60 per

MICROFILM

\$

0.86 per

jpl

JET PROPULSION LABORATORY  
CALIFORNIA INSTITUTE OF TECHNOLOGY  
PASADENA, CALIFORNIA

October 15/1962

23p

ref


Reproduced by  
NATIONAL TECHNICAL  
INFORMATION SERVICE  
Springfield, Va. 22151

NATIONAL AERONAUTICS AND SPACE ADMINISTRATION  
CONTRACT No. NAS 7-100

*Technical Report No. 32-226*  
*Revision No. 1*

*Optimum Interplanetary Rendezvous Trajectories  
with Power-Limited Vehicles*

*W. G. Melbourne*  
*C. G. Sauer, Jr.*

  
\_\_\_\_\_  
C. R. Gates, Chief  
Systems Analysis Section

JET PROPULSION LABORATORY  
CALIFORNIA INSTITUTE OF TECHNOLOGY  
PASADENA, CALIFORNIA

October 15, 1962

Copyright© 1962  
Jet Propulsion Laboratory  
California Institute of Technology

## CONTENTS

I. Introduction . . . . .	1
II. Optimum Thrust Equations . . . . .	2
III. Propulsion System Optimization . . . . .	3
IV. Missions and Terminal Conditions . . . . .	4
V. Interplanetary Trajectories . . . . .	5
VI. Comparison of Variable- and Constant-Thrust Programs . . . . .	12
Table 1. Differences Between Constant- and Variable-Thrust Programs for 184-Day Flight . . . . .	12
References . . . . .	14
Appendix. Analytical Basis for Thrust Equations . . . . .	15

## FIGURES

1. Mars rendezvous trajectories, 184-day flight time, variable-thrust program, ecliptic projection . . . . . 5
2. Mars rendezvous trajectories, 184-day flight time, constant-thrust program with optimum coast, ecliptic projection . . . . . 5
3. Earth-Mars rendezvous trajectories, variable-thrust program,  $\int_{t_0}^{t_1} a^2 dt$  ( $m^2/sec^3$ ) . . . . . 6
4. Earth-Mars rendezvous trajectories, variable-thrust program, flight time vs launch date for constant  $\int_{t_0}^{t_1} a^2 dt$  ( $m^2/sec^3$ ) . . . . . 7
5. Mars optimum rendezvous trajectories with equal  $\int_{t_0}^{t_1} a^2 dt$ , flight time and launch date, 184-day flight time, variable-thrust program . . . . . 8
6. Earth-Mars rendezvous trajectories, variable-thrust program,  $\int_{t_0}^{t_1} a^2 dt$ , vs launch date for constant flight time, 1968-1972 . . . . . 8
7. Earth-Mars rendezvous trajectories  $\int_{t_0}^{t_1} a^2 dt$  vs flight time for optimum and least-optimum rendezvous conditions . . . . . 9
8. Mars 1971 ballistic trajectories, sum of geocentric and areocentric hyperbolic excess speeds vs launch date for constant flight time . . . . . 11

**ABSTRACT**

13404

The optimum-thrust equations for both variable and constant thrust are presented. These thrust programs are used to generate rendezvous trajectories from the Earth to Mars for various flight times and launch dates during the years 1968-71. The manner in which the propulsion requirements vary with flight time and launch date are considered, and a comparison of vehicle performance using the variable- and constant-thrust programs is presented. The optimization of the propulsion system parameters is discussed, and the existence of optimum launch dates is interpreted in terms of certain transversality conditions derivable from the calculus of variations. A brief comparison of the advanced propulsion vehicle and the ballistic vehicle propulsion requirements is made for Earth-Mars rendezvous trajectories. An appendix considering the analytical basis for this work is included. *Author*

**I. INTRODUCTION**

The emergence of advanced propulsion for interplanetary flights has generated great interest in the application of optimization theory to advanced propulsion vehicle systems and to trajectory design. It becomes necessary to obtain fairly accurate estimates of the payload capabilities of advanced propulsion vehicles for various interplanetary missions. Results from a series of trajectories to the planets Venus and Mars appeared in Ref. 1. An optimum variable-thrust program was used to generate these trajectories.

Certain terminal conditions, moreover, such as the orientation of the terminal orbit and the terminal position on the orbit, were left unspecified and, instead, corresponding transversality conditions derived from the calculus of variations were satisfied.

This report considers the problem in which all end conditions, as determined by the planetary ephemerides, are specified, and its main purpose is to show the manner in which the propulsion requirements vary both with flight time and launch date. This procedure is analogous to the problem in ballistic trajectories of determining the velocity increments required for interplanetary missions (Ref. 2 and 3). In advanced propulsion trajectories, however, the propulsion intervals constitute a significant portion of the trajectory; therefore, the thrust program employed becomes quite important in payload studies, and optimization theory as applied to trajectory analysis is of considerable utility. A comparison of vehicle performance will be made between the use of an optimum variable-thrust program and an optimum constant-thrust program.

## II. OPTIMUM THRUST EQUATIONS

In order to develop an optimum-thrust program which extremizes some terminal quantity indicative of vehicle performance, it is necessary to include the constraints of the system. For the power-limited propulsion system the constraints are the equations of motion of the vehicle and an equation describing the fact that the amount of kinetic power contained in the exhaust propellant is constrained. Generally, the kinetic power depends on the efficiency of power conversion from the nuclear powerplant of the vehicle, and the efficiency, in turn, is dependent on the exhaust velocity employed. In this treatment, the kinetic power is constant, which is the case for the constant thrust program since the exhaust velocity is constant. The variable thrust program possesses a variable exhaust velocity; thus, performance figures obtained from this program are optimistic for two reasons: (1) the thrust program is unconstrained, and (2) the variation of efficiency is neglected. On the other hand, performance figures from the constant-thrust program tend to be conservative but are more realistic.

The constraining equations of motion are:

$$\ddot{\mathbf{r}} + \nabla V - \mathbf{a} = \mathbf{0} \quad (1)$$

and the power-limited constraint is

$$\dot{\mu} + \frac{\beta}{c^2} \alpha_p = 0 \quad (2)$$

where  $\mathbf{r}$  is the position vector of the vehicle,  $V$  is the potential of the force field,  $\mathbf{a}$  is the thrust acceleration with the magnitude

$$a = -\dot{\mu} \frac{c}{\mu} = \frac{\beta}{\mu c} \alpha_p \quad (3)$$

The quantity  $\mu$  is the normalized mass of the vehicle [ $\mu(t_0) = 1$ ],  $\beta$  is twice the kinetic power in the rocket

exhaust per unit initial mass of the vehicle and is, therefore, a constant dependent on the specific mass and size of the powerplant. The quantity  $c$  is the exhaust velocity, and  $\alpha_p$  is a switching parameter with the value 1 during propulsion periods and 0 during coasting periods.

A Mayer formulation (see Ref. 4 and 5) of the calculus of variations has been applied to both the constant and variable thrust cases to obtain the optimum thrust equations. The optimum thrust equations are (see Appendix):

$$\ddot{\boldsymbol{\lambda}} + (\boldsymbol{\lambda} \cdot \nabla) \nabla V = \mathbf{0}, \quad (4)$$

$$\mathbf{a} = \begin{cases} \text{constant } \boldsymbol{\lambda}, \text{ variable thrust} \\ \frac{\text{constant}}{\mu} \frac{\boldsymbol{\lambda}}{\lambda} \alpha_p, \text{ constant thrust} \end{cases} \quad (5)$$

where  $\boldsymbol{\lambda}$  is the Lagrange multiplier vector, and the constant in Eq. (5) is determined from boundary conditions. It may be shown that no coasting periods occur in the variable-thrust program (Ref. 5, 6, and 7). In the constant-thrust program the switching function  $L(t)$ , generated by the equation

$$L = \frac{\lambda}{\mu} \quad (6)$$

determines the periods of propulsion and coast by the conditions

$$\begin{aligned} L > 0, \alpha_p &= 1 \\ L < 0, \alpha_p &= 0 \end{aligned} \quad (7)$$

In the case where  $V$  is explicitly independent of time it may be shown that the equations of motion (Eq. 1) and the Euler equations (Eq. 4) possess a first integral in the form

$$\begin{aligned} \dot{\boldsymbol{\lambda}} \cdot \dot{\mathbf{r}} + \boldsymbol{\lambda} \cdot \nabla V - \frac{1}{2} a \lambda &= K_2, \text{ variable thrust} \\ \dot{\boldsymbol{\lambda}} \cdot \dot{\mathbf{r}} + \boldsymbol{\lambda} \cdot \nabla V - a \mu L &= K_2, \text{ constant thrust} \end{aligned} \quad (8)$$

### III. PROPULSION SYSTEM OPTIMIZATION

By eliminating  $c$  from Eq. (2) and (3) and integrating, one obtains

$$\frac{1}{\mu_1} = \frac{1}{\mu_0} + \int_{t_0}^{t_1} \frac{a^2}{\beta} dt \quad (9)$$

the so-called rocket equation for power-limited propulsion systems. The quantity

$$J = \int_{t_0}^{t_1} a^2 dt \quad (10)$$

appearing in Eq. (9) is analogous to the concept of characteristic velocity in chemical rocket trajectories and is a convenient index of rocket performance. Since in this treatment,  $\beta$  remains constant, any thrust program maximizing  $\mu_1$  also minimizes  $J$ . In the variable thrust program the exhaust velocity is determined through Eq. (2), (3), and (5). In the constant-thrust program, for a particular mission, any exhaust velocity below some maximum value yields an optimum trajectory. These trajectories possess different lengths of coasting and dif-

ferent values of  $J$ . There exists in general, an optimum exhaust velocity yielding a minimum  $J$ . It is shown in Ref. 5 and the Appendix that the condition

$$\int_{t_0}^{t_1} a_p \left( 2L - \frac{\lambda}{\mu} \right) dt = 0 \quad (11)$$

guarantees an extremal in  $J$  with respect to the exhaust velocity for the constant-thrust program.

It turns out that  $J_{\min}$  is nearly invariant to the value of  $\beta$  for feasible missions (Ref. 5), which is its principal asset as an index of rocket performance. In particular, by fixing  $c$  and finding the optimum initial thrust acceleration which minimizes  $J$  one obtains nearly the same value of  $J_{\min}$  (generally within 1%). The condition for an extremal in  $J$  for this process is given by

$$\left[ \mu (\lambda - \mu L) \right]_{t_0}^{t_1} = 0 \quad (12)$$

Both procedures as indicated in Eq. (11) and (12) have been employed in the numerical results to follow.



## IV. MISSIONS AND TERMINAL CONDITIONS

The position and velocity coordinates must satisfy specified values or functions at both end points of the rendezvous trajectory. In planetary-rendezvous missions, six terminal quantities must be specified at each end point. In Ref. 1, it was described how these quantities were grouped into five orbital quantities which determine the shape and orientation of the terminal ellipse and are essentially time-invariant, and one time-varying quantity indicating the rendezvous position on the terminal ellipse. A description of these quantities is contained in Ref. 1.

It was also shown in Ref. 1 and 5 (see Appendix) that for each terminal condition left unspecified there results a corresponding transversality condition to be satisfied at the end point, instead. Satisfying these transversality conditions yields extremals in the quantity being optimized with respect to the unspecified terminal conditions. In particular, it was shown that if the rendezvous position (true anomaly, say) on the terminal ellipse is left unspecified at either end point the transversality condition

$$\dot{\lambda} \cdot \dot{\mathbf{r}} + \lambda \cdot \nabla V = 0 \quad (13)$$

should be satisfied at the corresponding end point(s). If, in addition, the transfer angle between the initial and

final point of the trajectory is unspecified then the z-component of the constant vector  $\mathbf{K}_1$ , given by

$$\mathbf{K}_1 = \mathbf{r} \times \dot{\lambda} - \dot{\mathbf{r}} \times \lambda \quad (14)$$

must be zero.

The z-direction is perpendicular to the plane containing the transfer angle (the angle  $\theta$  as defined in Ref. 1). Equation (14) holds in any central force field and the z-component of  $\mathbf{K}_1$ , is the same constant  $K_1$ , appearing in Ref. 1 in the spherical coordinate formulation of the Euler-Lagrange equations. These two transversality conditions will be used to interpret the behavior of the performance requirements with launch date. One further transversality condition will be used in the sequel. Suppose the initial and final conditions are determined by ephemerides and are, therefore, functions only of the launch and arrival dates, respectively. It is shown in the appendix that if the launch date  $t_0$ , is unspecified for a fixed flight time, satisfying the transversality condition

$$\left[ \dot{\lambda} \cdot \dot{\mathbf{r}} + \lambda \cdot \nabla V \right]_{t_0}^{t_1} = 0 \quad (15)$$

yields an extremal in the quantity being optimized with respect to launch date.

## V. INTERPLANETARY TRAJECTORIES

The optimum-thrust equations, the constraining equations, and various ancillary equations have been programmed in three dimensions for numerical solution on an IBM 7090. Equation (8) is used to check the accuracy of the numerical integrations. A Newton-Raphson (Ref. 8) search method has been used to obtain converged trajectories with specified boundary conditions. By the use of this method in conjunction with certain prediction schemes (Ref. 8) it has been possible to generate wholesale amounts of trajectories with only a moderate consumption of machine time. By this technique, the indirect method of the calculus of variation has been eminently successful when applied to interplanetary trajectories, even in three dimensions where six and sometimes seven quantities are specified at the final point.

The results from a series of three-dimensional rendezvous trajectories from Earth to Mars are presented. These trajectories utilize the actual positions and velocities of these planets during the era 1968-1971 as initial and final conditions. Only the gravitational field of the Sun was included in these calculations. As an example of the nature of these trajectories Fig. 1 shows three trajectories of the same flight time launched at different dates during the synodic era, 1970-1971. The variable thrust

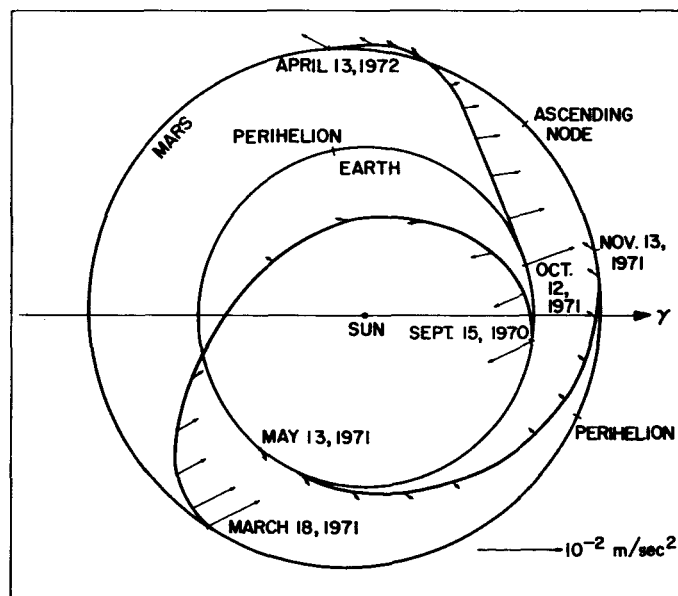


Fig. 1. Mars rendezvous trajectories, 184-day flight time, variable-thrust program, ecliptic projection

program was used to generate these trajectories, and the arrows on the trajectories indicate the direction and magnitude of the thrust acceleration. This figure is an ecliptic projection; the effect of the third dimension is small and has been discussed in Ref. 1. Figure 2 shows the same trajectories generated by the constant thrust-program, and the similarities should be noted. These trajectories possess an optimum coast period in the sense that Eq. (11) is satisfied for a fixed value of  $\beta$  of  $100.0 \text{ m}^2/\text{sec}^3$ ; the periods of coast have been indicated. The 9/15/70 and 10/12/71 trajectories are probably not feasible missions; the thrust acceleration vector at the final point of these two trajectories in Fig. 2 has increased to about twice the size of the initial value, indicating that about half the vehicle mass has been depleted. This is about the maximum mass loss that can be sustained by an advanced propulsion vehicle and still deliver a significant payload.

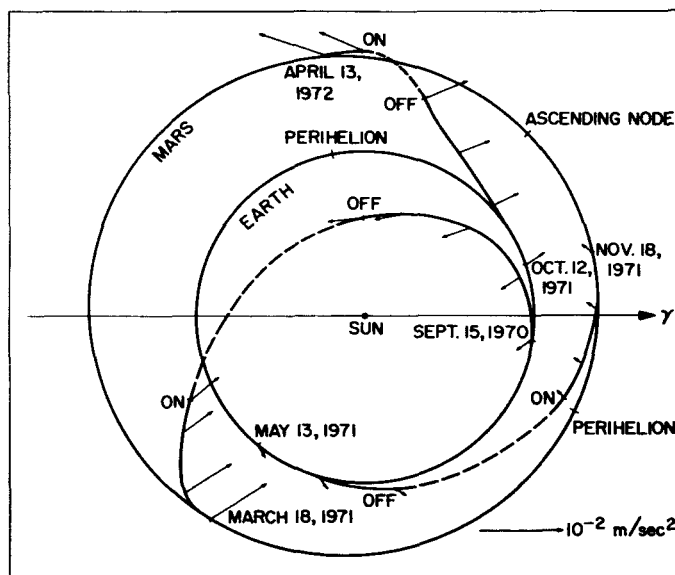


Fig. 2. Mars rendezvous trajectories, 184-day flight time, constant-thrust program with optimum coast, ecliptic projection

A series of trajectories with different launch dates and flight times has been obtained. Figure 3 shows the variation of  $J$  with heliocentric launch date for many flight times using the variable-thrust program. With these figures it is possible to determine the "launch period" which is available for given maximum value of  $J$  and a specified range of flight times. At the launch date where mini-

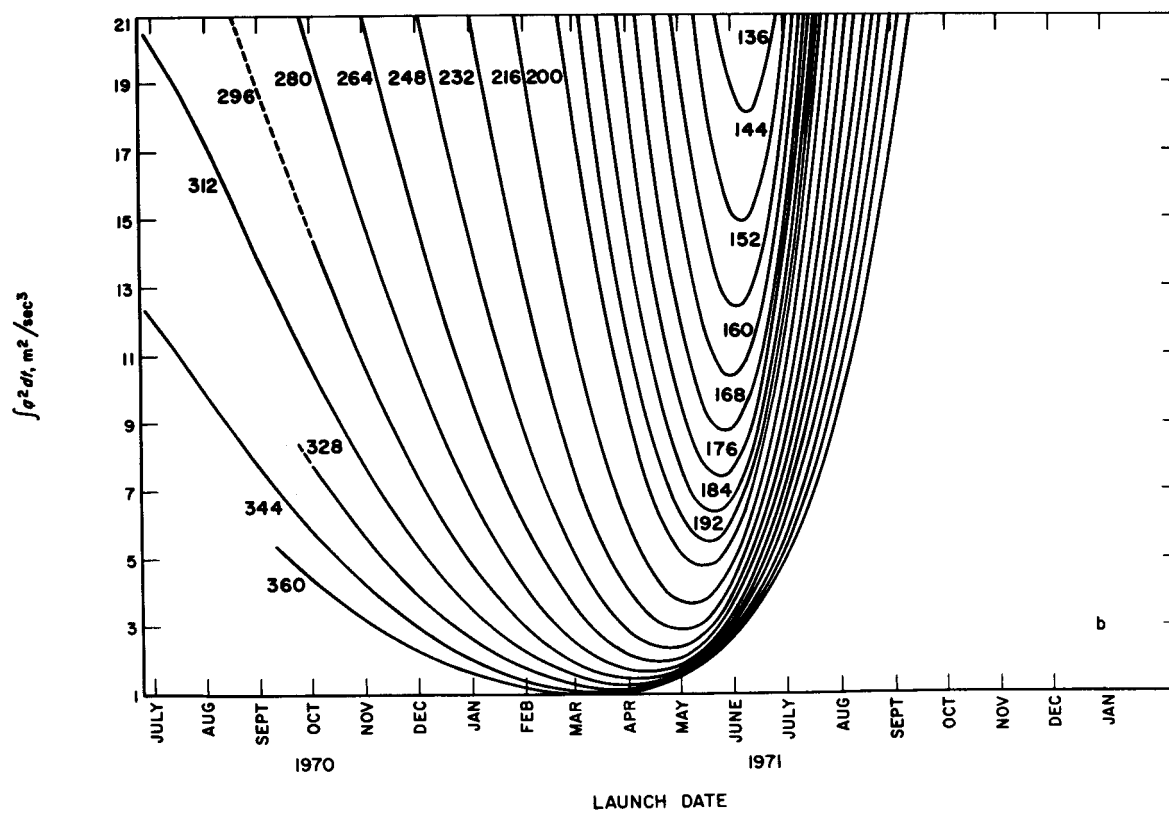
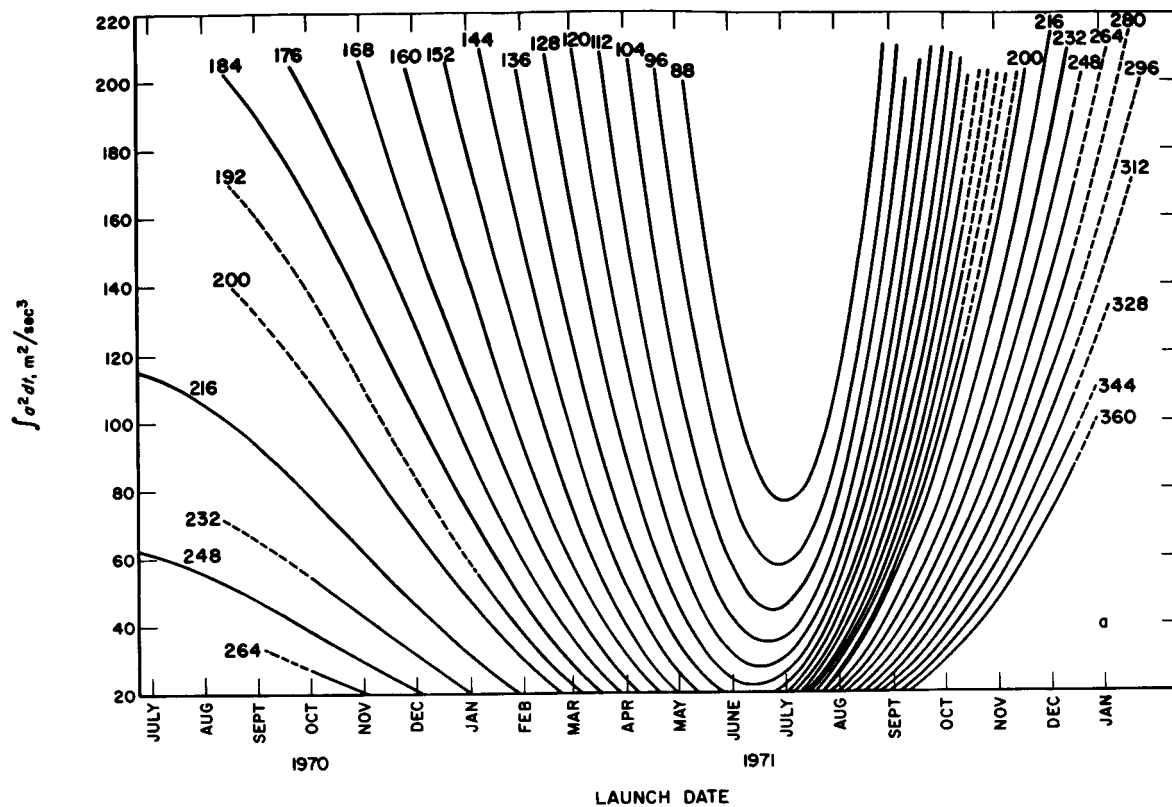


Fig. 3. Earth-Mars rendezvous trajectories, variable-thrust program,  $\int_{t_0}^t a^2 dt (m^2/sec^3)$

imum  $J$  occurs for a given flight time, the transversality condition in Eq. (15) is satisfied. The 5/13/71 trajectory shown in Fig. 1 and 2 has nearly the optimum launch date for a 184-day flight time and for this synodic era.

Figure 4 exhibits contours of equal  $J$  with flight time versus heliocentric launch date. The minima of these curves correspond to minimum-time trajectories for a given value of  $J$  and the transversality condition in Eq. (15) is also satisfied at this point. The locus of minimum flight for a given  $J$  will pass, for zero flight time, near the date of Earth-Mars opposition which is about 8/10/71.

The curves in Fig. 3 are not unique because there exist classes of trajectories yielding extremals in  $J$  which, for a given launch date and flight time, rendezvous Mars

after executing an arbitrary number of circuits around the Sun either in the forward or retrograde directions. Of particular interest is that class of trajectories making one less circuit around the Sun and which corresponds to the optimum set in the preceding synodic era of 1969, just as the ones shown are optimum for the 1971 era. For a given flight time there clearly exists a launch date which is a trade-off point and which, for earlier dates, the optimum path is obtained by subtracting  $2\pi$  from the transit angle required to rendezvous Mars. Figure 5 shows an example from each of these two classes of trajectories using a variable thrust program. Both of these trajectories have the same flight time and possess the same value of  $J$  but utilize radically different thrust programs in carrying out the mission.

Figure 6 is a semi-log plot of  $J$  versus launch date for both the 1969 and 1971 synodic eras. Both classes of tra-

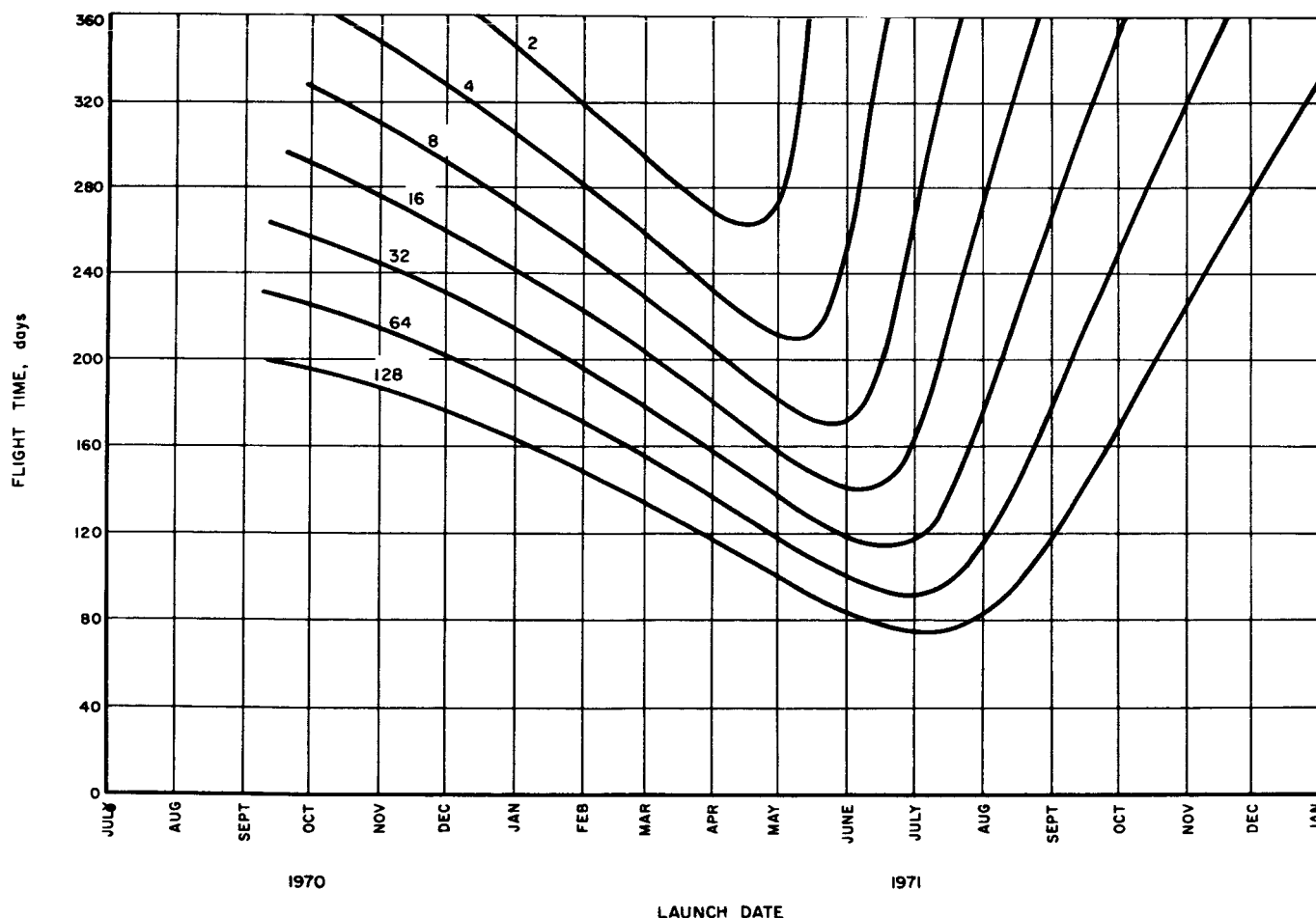


Fig. 4. Earth-Mars rendezvous trajectories, variable-thrust program, flight time vs launch date for

$$\text{constant } \int_{t_0}^t a^2 dt \text{ (m}^2/\text{sec}^2\text{)}$$

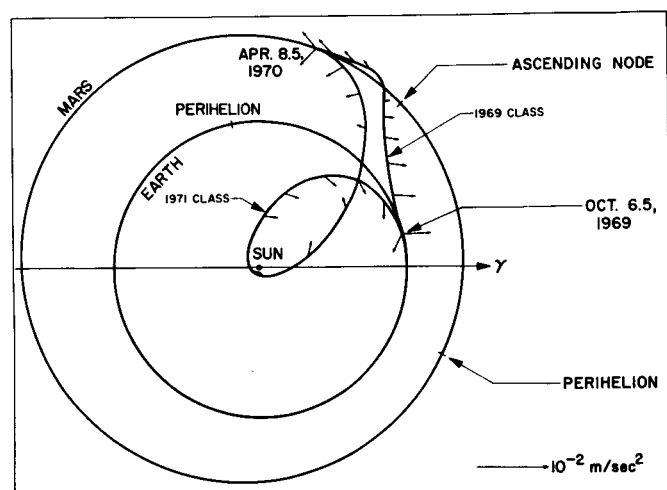


Fig. 5. Mars optimum rendezvous trajectories with equal  $\int_0^t a^2 dt$ , flight time and launch date, 184-day flight time, variable-thrust program

jectories are shown on this figure, and the trade-off points in launch date are clearly seen. The trajectories of the left-hand wing of the 1971 class appearing in 1969-70 in Fig. 6 are probably of academic interest only since the values of  $J$  for these curves are so high. For the presently estimated state-of-the-art of advanced propulsion technology, missions with values of  $J$  greater than around  $50 \text{ m}^3/\text{sec}^2$  are probably not feasible. The local extremals in  $J$  with launch date which appear in the wings also fulfill the condition in Eq. (15). These trajectories, typically, fall in toward the Sun upon leaving the Earth, making a circuit around the Sun and then head out toward Mars.

The increased steepness on the ascending branches of these curves may be explained in terms of the decreasing transit angle of the trajectory with increasing launch date as shown in Fig. 1 and 2. For launch dates past

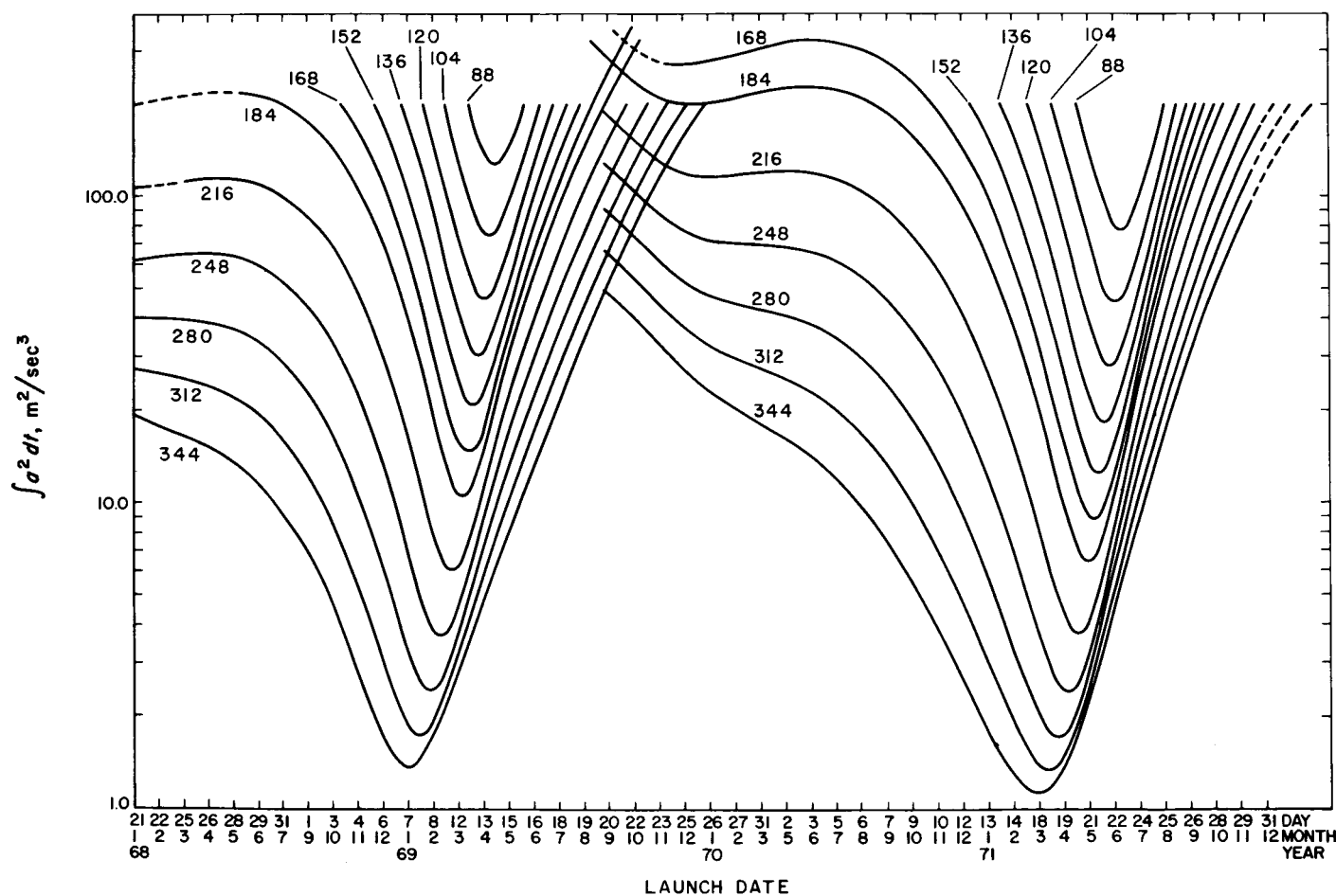


Fig. 6. Earth-Mars rendezvous trajectories, variable-thrust program,  $\int_0^t a^2 dt$  vs launch date for constant flight time, 1968-1972

the optimum point the percentage change in transit angle is greater than for equally distant launch dates preceding the optimum point. As the positions of Earth at launch and Mars at arrival approach opposition, a more radical thrust program (as indicated in the 10/11/71 trajectory) than the program for optimal transfer is required. This same effect occurs in ballistic trajectories.

The year 1971 is a "vintage year" for advanced propulsion trajectories (and also ballistic trajectories) in the sense that the minima of these curves possess smaller values for this year than they do for immediately preceding or succeeding synodic eras. Notice in Fig. 6 that the minima in 1969 lie at a higher value of  $J$  than do the corresponding minima in 1971. This phenomenon can be interpreted in terms of the fact that for 1971, the transversality condition in Eq. (13) is nearly satisfied for all flight times at both the initial and final points of the trajectory at the optimum launch dates. Searching for the optimum synodic era is tantamount to removing the coupling supplied by the ephemerides between planetary positions and launch and arrival dates. In this case, the positions on the initial and final ellipses become unspecified, and Eq. (15) decomposes into Eq. (13) which must be satisfied at both terminal points. (See Appendix.) In 1971 the Earth-Mars distance at opposition is smaller than in neighboring synodic eras—this phenomenon repeats approximately every fifteen years, or every seven synodic periods. It is known, however, that the optimum point of rendezvous at Mars is not at perihelion but rather at some point past perihelion where the radial velocity is, in general, outward (see Ref. 9).

In order to isolate the range of variation of minimum  $J$  with synodic era, a series of trajectories was run in which the transversality condition in Eq. (13) was satisfied at both terminal points. Since the orbit of the Earth is nearly circular, this approximation was made in these computations. In this case, it can be shown (see Appendix) that Eq. (13) implies that the  $z$ -component of  $\mathbf{K}_1$  is zero simplifying the analysis, somewhat. Figure 7 shows the variation in  $J$  with flight time for Mars rendezvous trajectories in which Eq. (13) is satisfied at the final point of the trajectory and the constant  $K_{1z}$  is zero. Both local minima and local maxima occur when these conditions are satisfied. The lower triplet of curves corresponds to rendezvous at the optimum orbital point and the upper set corresponds to rendezvous at the least optimum point, which generally is approximately 180 deg away from the optimum point. The optimum rendezvous points are functions of flight time (Ref. 9). The varia-

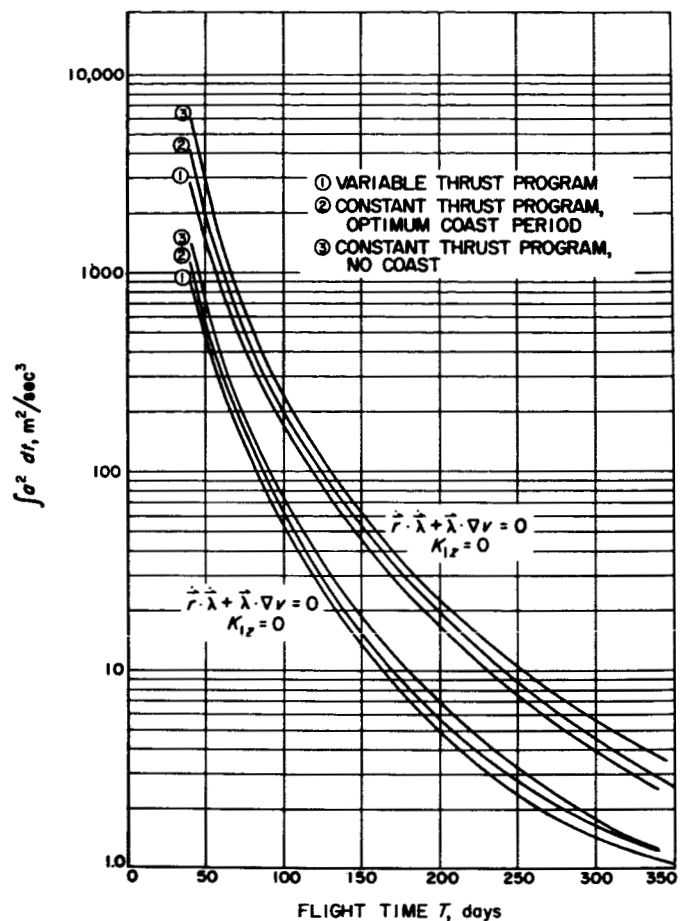


Fig. 7. Earth-Mars rendezvous trajectories  $\int_{t_0}^{t_1} a^2 dt$  vs flight time for optimums and least-optimum rendezvous conditions

tions of  $J$  with flight time using a constant thrust program with optimum coast and no coast are also shown on this figure and will be discussed shortly. The upper and lower variable thrust curves shown on Fig. 7 bound the range of variation of minimum  $J$  with synodic period using a variable thrust program. It should be observed that the minima of the 1971 curves lie almost exactly along the lower curve in Fig. 7. At three or four synodic periods before or after 1971, the Earth-Mars configuration at optimum launch date is such that trajectories rendezvous near the least optimum point and the minima therefore lie near the upper variable thrust curve in Fig. 7.

The estimates of propellant requirement for heliocentric transfer as given in Fig. 3 through 6 tend to be slightly conservative because of the neglect of the masses of the departure and arrival planets. In spiralling away

## REVISION NO. 1

from the Earth, for example, the geocentric velocity at escape is, typically, around 1 km/sec. It may be shown (Ref. 9) that the velocity at escape is proportional to the fourth root of the thrust acceleration and the gravitational constant of the central planet, so the velocity at escape changes little with the thrust acceleration employed. In any case, this velocity, although small compared to the 30 km/sec orbital velocity of the Earth, can be used, if properly directed, to obtain a reduction in the  $J$  required for the heliocentric portion of the flight. Preliminary studies suggest that approximately 15% reduction in  $J$  for the heliocentric flight can be obtained by taking the masses of the departure and arrival planets into account.

Finally, it is interesting to compare the propulsion requirements for an advanced propulsion vehicle with those for a ballistic vehicle. Figure 8 shows the sum of the geocentric and Mars-centered hyperbolic-excess speeds versus launch date for various flight times. This figure is obtained from results appearing in Ref. 3 in which heliocentric conics were fitted through the Earth and Mars as explained in Ref. 2 and 3. The similarities between Fig. 3 and 8 should be noted. For a given flight time, the optimum launch dates are approximately the same for the two types of trajectories discussed; however, the "firing period" for the advanced propulsion vehicle is somewhat wider than the "firing period" for the ballistic vehicle.

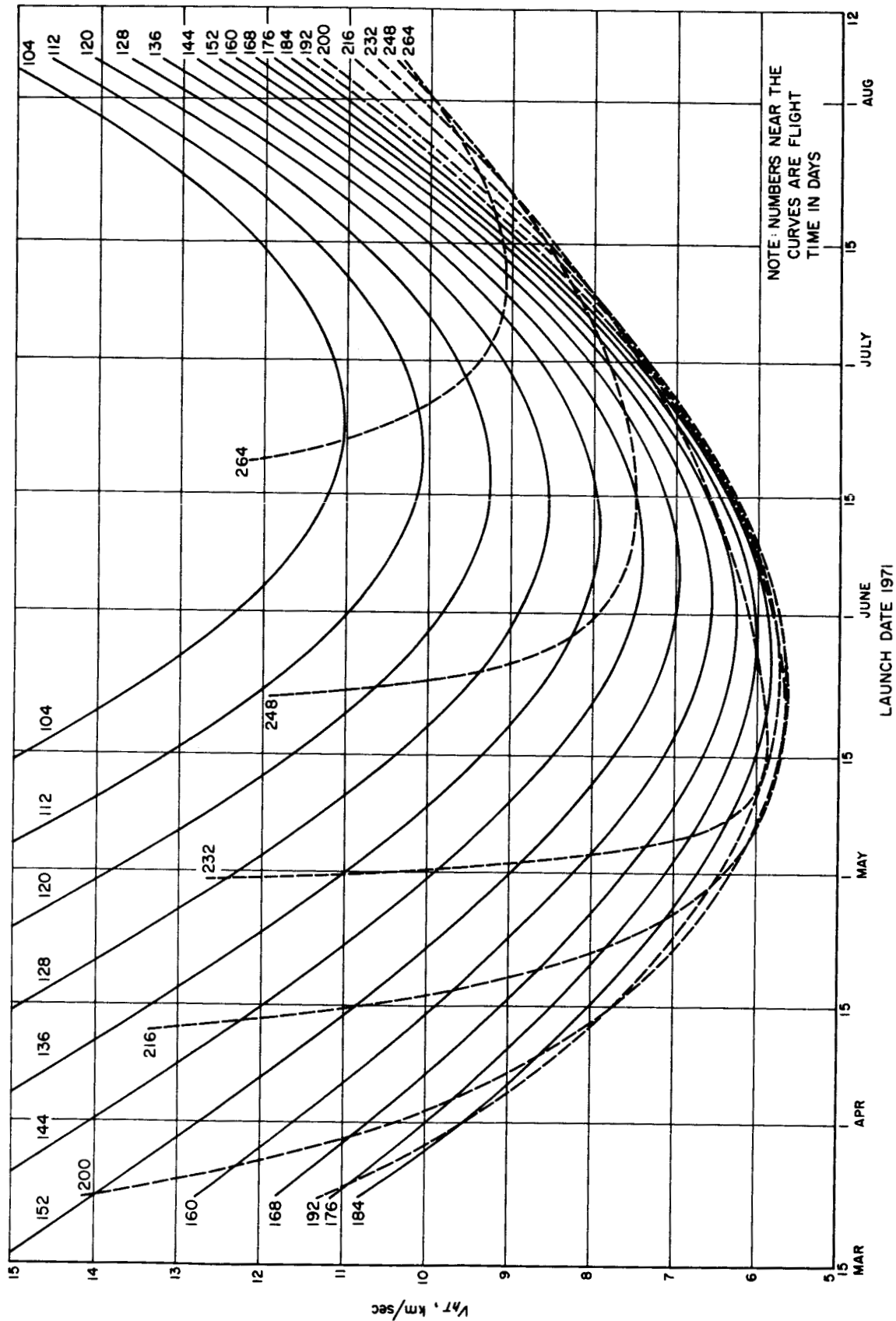


Fig. 8. Mars 1971 ballistic trajectories, sum of geocentric and areocentric hyperbolic excess speeds vs launch date for constant flight time



## VI. COMPARISON OF VARIABLE- AND CONSTANT-THRUST PROGRAMS

From the curves in Fig. 7 the degradation in vehicle performance resulting from using a less optimum thrust program is easily assessed. The constant-thrust curves were generated using a fixed exhaust velocity of 50,000 m/sec. The optimum coast curves were obtained by satisfying Eq. (12). As stated earlier,  $J$  is insensitive for feasible missions to the values of  $c$  or  $\beta$  employed, varying less than 10% for missions with more than about half the mass of the vehicle remaining at the final point (see Table 1 or consult Ref. 5). In this figure the increase in  $J$  in the constant-thrust program with optimum coast is about 15% over the variable thrust program. This corresponds, typically, to about a 3% decrease in  $\mu$ , as may be verified from Eq. (9); that is, for small variations

$$\delta\mu_1 = -\mu_1 (1 - \mu_1) \frac{\delta J}{J} \quad (16)$$

For trajectories launched at dates other than the optimum launch date, the percentage difference in  $J$  between the two thrust programs varies somewhat but ranges from 10 to 30%. Table 1 illustrates the difference between these two programs for various launch dates for a 184-day flight. The transversality condition in Eq. (11) is satisfied in the constant-thrust program using values for  $\beta$  of 100 m<sup>2</sup>/sec<sup>3</sup> and infinity (constant-thrust acceleration). In addition, the results from a corresponding set of two-dimensional trajectories are presented to show the difference between two and three-dimensional analysis for interplanetary trajectories. The differences are small as already pointed out in Ref. 1. The largest effect occurs near the optimal launch date which reflects the fact that the additional propulsion requirement for the out-of-the ecliptic dimension is relatively insensitive to the launch date.

The variable-thrust program has been used in the majority of the numerical computations for several reasons. The performance results constitute a unique upper bound independent of the propulsion system design; the computation time is generally less than with the constant thrust program because (1) the dimension of the iteration matrix is smaller since no propulsion system optimization is required and (2) the variable-thrust equations seem somewhat more stable, computationally, and converge more rapidly. The use of a constant-thrust acceleration program (infinite  $\beta$ ) with optimum coast

Table 1. Differences between constant- and variable-thrust programs for 184-day flight

Launch date (1971)	Constant thrust			Variable thrust $\int a^2 dt$
	$\int a^2 dt$ $\beta = \infty$	$\int a^2 dt$ $\beta = 100.0$	$\mu_1$ $\beta = 100.0$	
Three-dimensional trajectories				
2/14	45.477	43.131	0.699	37.373
3/2	33.980	32.406	0.755	27.733
3/18	24.608	23.640	0.809	19.931
4/3	17.298	16.757	0.856	13.938
4/19	11.949	11.678	0.895	9.703
5/5	8.516	8.404	0.922	7.187
5/13	7.596	7.546	0.930	6.576
5/21	7.340	7.351	0.932	6.406
6/6	8.966	9.110	0.917	7.459
6/22	13.180	13.565	0.881	10.558
7/8	20.150	21.070	0.826	16.046
7/24	30.417	32.479	0.755	24.395
8/9	44.691	49.038	0.671	36.217
8/17	53.583	59.766	0.626	43.648
Two-dimensional trajectories				
2/14	45.165	42.864	0.700	37.230
3/2	33.714	32.171	0.757	27.597
3/18	24.379	23.431	0.810	19.796
4/3	17.096	16.567	0.858	13.798
4/19	11.762	11.498	0.897	9.555
5/5	8.334	8.225	0.924	7.032
5/13	7.414	7.364	0.931	6.418
5/21	7.161	7.171	0.933	6.247
6/6	8.801	8.942	0.918	7.303
6/22	13.023	13.401	0.882	10.413
7/8	20.003	20.914	0.827	15.918
7/24	30.289	32.339	0.756	24.292
8/9	44.588	48.920	0.672	36.139
8/17	53.492	59.659	0.626	43.584

also has the advantages of being independent of the propulsion system design and yields more conservative performance results. Experience has shown that this program is nearly as stable and economical as the variable-thrust program and requires only one additional dimension in the iteration matrix, namely, the fulfillment of Eq. (12) at the final point of the trajectory. The present policy at JPL in parametric mission feasibility studies is to employ both of these programs to obtain performance figures which bracket the performance capabilities of an actual advanced propulsion vehicle.

## ACKNOWLEDGEMENT

The authors wish to express their sincere gratitude to D. E. Richardson, who collaborated in the development of the computer program, and to Mrs. Helen Ling for her assistance in the numerical results.

## REFERENCES

1. Melbourne, W. G., "Three-Dimensional Optimum Thrust Trajectories for Power-Limited Propulsion Systems," *ARS Journal*, Vol. 31, No. 12, December 1961.
2. Breakwell, J. V., Gillespie, R. W., and Ross, S., "Researches in Interplanetary Transfer," *ARS Journal*, Vol. 31, No. 2, February 1961, pp. 201-208.
3. Clarke, V. C., Bollman, W. E., and Scholey, W. J., *Design Parameters for Ballistic Interplanetary Trajectories—Part I, One-Way Transfer to Mars and Venus*, Technical Report 32-77, Jet Propulsion Laboratory, Pasadena, California, March 1, 1962.
4. Bliss, G. A., *Lectures on the Calculus of Variations*, The University of Chicago Press, Chicago, Illinois, 1946, Ch. 1 and 7.
5. Melbourne, W. G., and Sauer, C. G., Jr., *Optimum Thrust Programs for Power-Limited Propulsion Systems*, Technical Report No. 32-118, Jet Propulsion Laboratory, Pasadena, California, 1961 (also *Astronautica Acta*, in press).
6. Irving, J. H., *Space Technology*, ed. H. S. Seifert, Wiley and Sons, New York, 1959, Ch. 10.
7. Leitman, G., "Minimum Transfer Time for a Power-Limited Rocket," *Applied Mechanics Journal*, Vol. 28, June 1961, pp. 171-178.
8. Melbourne, W. G., Richardson, D. E., and Sauer, C. G., *Interplanetary Trajectory Optimization with Power-Limited Vehicles*, Technical Report 32-173, Jet Propulsion Laboratory, Pasadena, California, 1961.
9. Melbourne, W. G., *Interplanetary Trajectories and Payload Capabilities of Advanced Propulsion Vehicles*, Technical Report 32-68, Jet Propulsion Laboratory, Pasadena, California, March 31, 1961.

## APPENDIX

## Analytical Basis for Thrust Equations

The analytical basis for most of the equations appearing in the text has been discussed in Ref. 5 and will, consequently, only be reviewed at this time with the emphasis being placed on new results. A Mayer formulation (Ref. 4) of the calculus of variations has been applied to the problem of obtaining the optimum thrust equations which extremize some function of the end conditions.

Let  $q_j(t)$  denote both the state and the control variables of the problem ( $j = 1, 2, \dots, n$ ). Let the constraining relations be denoted by the functions

$$G_i(q_j, \dot{q}_j, t, t_0, t_1, \kappa_v) = 0 \quad i = 1, 2, \dots, m < n \quad (\text{A-1})$$

and let  $\lambda_i(t)$  be a set of time-dependent Lagrange multipliers. Let  $F$  be a function defined by

$$F = \lambda_i G_i \quad (\text{A-2})$$

where the summation rule is employed. The quantity to be extremized is given by

$$J = J(q_j(t_1), q_j(t_0), t_0, t_1, \kappa_v) \quad (\text{A-3})$$

that is, a function of the variables at the end points only and an arbitrary number of parameters  $\kappa_v$  ( $v = 1, 2, \dots, r$ ). As necessary conditions for extremizing  $J$ , the  $q_j$  must satisfy the Euler-Lagrange equations given by

$$\frac{d}{dt} \left( \frac{\partial F}{\partial \dot{q}_j} \right) - \frac{\partial F}{\partial q_j} = 0, \quad j = 1, 2, \dots, n \quad (\text{A-4})$$

at all points along the trajectory except at corners, i.e., points of discontinuity in one or more of the  $q_j$ . Further, at such corners the Weierstrass-Erdmann corner conditions must hold, namely,

$$\frac{\partial F}{\partial \dot{q}_j} \text{ is continuous} \quad j = 1, 2, \dots, n \quad (\text{A-5})$$

$$F - \frac{\partial F}{\partial \dot{q}_j} \dot{q}_j \text{ is continuous} \quad (\text{A-6})$$

If the constraining functions are not explicit functions of time, a first integral of the Euler-Lagrange equation is

$$F - \frac{\partial F}{\partial \dot{q}_j} \dot{q}_j = \text{constant} \quad (\text{A-7})$$

One additional tool from the calculus of variations will be needed in dealing with corners, namely, the Weier-

strass  $E$ -function. This function yields a further necessary condition for the minimization of  $J$  by the inequality

$$E = F(q_1^*, \dots, q_n^*, \dot{q}_1^*, \dots, \dot{q}_n^*) - F(q_1, \dots, q_n, \dot{q}_1, \dots, \dot{q}_n) - (\dot{q}_j^* - \dot{q}_j) \frac{\partial F}{\partial \dot{q}_j} \geq 0 \quad (\text{A-8})$$

The  $q_j^*$  is an admissible value in the vicinity of  $q_j$ . For continuous variables  $q_j^* = q_j$ ; however, for discontinuous variables  $q_j^*$  may take on any value consistent with the specified bounds. Using the constraining relations in Eq. (1) and (2), (with Eq. 1 replaced by two first-order equations) in conjunction with the above theory one obtains the optimum thrust equations as described by Eq. (4) through (8). The variable-thrust program is obtained by allowing  $c$  to be an unconstrained variable, the constant thrust program results from holding  $c$  fixed.

## A. Transversality Conditions

Since  $J$  possesses an extremal value it follows that the first variation of  $J$

$$\begin{aligned} dJ = & \frac{\partial J}{\partial t_0} dt_0 + \frac{\partial J}{\partial t_1} dt_1 + \frac{\partial J}{\partial q_i(t_0)} dq_i(t_0) \\ & + \frac{\partial J}{\partial q_i(t_1)} dq_i(t_1) + \frac{\partial J}{\partial \kappa_v} d\kappa_v = 0 \end{aligned} \quad (\text{A-9})$$

The terminal variations,  $dt_0$ ,  $dt_1$ ,  $dq_i(t_0)$ ,  $dq_i(t_1)$  and  $d\kappa_v$  are not independent but are related through the constraining equations and certain additional boundary conditions expressed in the form

$$A_j(q_i(t_1), q_i(t_0), t_1, t_0, \kappa_v) = 0, \quad j = 1, 2, \dots, p \leq 2n + r + 1 \quad (\text{A-10})$$

It follows that

$$\begin{aligned} & \frac{\partial A_j}{\partial t_0} dt_0 + \frac{\partial A_j}{\partial t_1} dt_1 + \frac{\partial A_j}{\partial q_i(t_0)} dq_i(t_0) \\ & + \frac{\partial A_j}{\partial q_i(t_1)} dq_i(t_1) + \frac{\partial A_j}{\partial \kappa_v} d\kappa_v = 0 \end{aligned} \quad (\text{A-11})$$

If the rank of the system of linear equations in the variations appearing in Eq. (A-9) and (A-11) is  $2n + r + 2$ , then the problem is essentially one with fixed end-points. If the boundary conditions, constraining equations, and parameters are compatible so that a solution exists, there is an optimum solution (or, at least a stationary one) for which  $J$  is extremized. The solution of the differential equations in Eq. (A-1) and (A-4) in conjunction with

## REVISION NO. 1

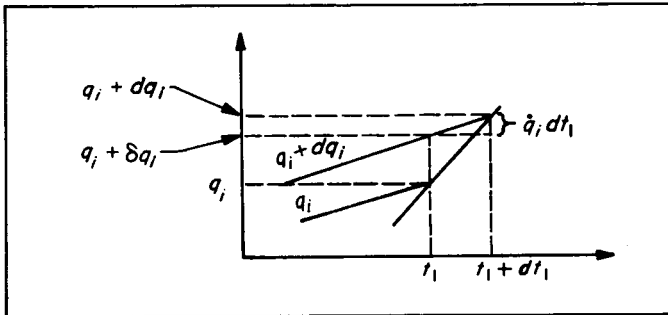
Eq. (A-3) and (A-10) serves to completely define the problem in this case and no further optimization is available.

On the other hand, a rank of Eq. (A-9) and (A-11) which is less than  $2n + r + 2$  implies that the boundary values of certain variables are undetermined and further extremization of  $J$  may be accomplished by choosing the appropriate values for the undetermined boundary values. The Euler-Lagrange equations were obtained from setting the first variation of  $\int_{t_0}^{t_1} F dt$  to zero and it follows at the terminal points<sup>1</sup>

$$\left[ F dt \right]_{t_0}^{t_1} + \int_{t_0}^{t_1} \left( \frac{\partial F}{\partial q_i} \delta q_i + \frac{\partial F}{\partial \dot{q}_i} \delta \dot{q}_i + \frac{\partial F}{\partial \kappa_v} d\kappa_v \right) dt =$$

$$\left[ \left( F dt + \frac{\partial F}{\partial \dot{q}_i} \delta q_i \right) \right]_{t_0}^{t_1} + \int_{t_0}^{t_1} d\kappa_v \frac{\partial F}{\partial \kappa_v} dt = 0 \quad (\text{A-12})$$

The  $\delta$ -variation is obtained while  $t$  is held fixed and consequently (see Sketch A) at a terminal point



$$\delta q_i = dq_i - \dot{q}_i dt \quad (\text{A-13})$$

and the condition for extremality to be satisfied at the boundaries becomes

$$\left[ \left( F - \frac{\partial F}{\partial \dot{q}_i} \dot{q}_i \right) dt + \frac{\partial F}{\partial \dot{q}_i} dq_i \right]_{t_0}^{t_1} + d\kappa_v \int_{t_0}^{t_1} \frac{\partial F}{\partial \kappa_v} dt = 0 \quad (\text{A-14})$$

Equation (A-14) is the classical transversality condition (see Ref. 4) with the additional integral term due to the parameters  $\kappa_v$ ; it assumes a nontrivial form when the rank of the boundary conditions is less than  $2n + r + 1$ .

<sup>1</sup>Although the term  $F dt$  in Eq. (A-12) is identically zero in the Mayer formulation, it is formally retained here since this analysis is applicable with little modification to the Lagrange and Bolza formulations where, in general, this term is nonzero.

The simultaneous solution of Eqs. (A-9), (A-11), and (A-14) yields the conditions on the terminal quantities resulting in an extremal in  $J$ . If certain terminal quantities are undetermined there results a corresponding transversality expression, in effect, for each absent terminal quantity. Satisfying a transversality expression yields an extremal in  $J$  with respect to the corresponding absent terminal quantity. An expedient way to solve this system of equations is to adjoin Eq. (A-9) and (A-11) to Eq. (A-14) in the usual manner through the use of Lagrange multiplier constants (see Ref. 5).

### B. Propulsion System Optimization

The above theory will now be used to present a derivation of Eq. (12) and (13) which differs, somewhat, from the method employed in Ref. 5. For the constant-thrust program and for a specified value of  $\beta$  there exists, in general, an optimum value of the parameter,  $c$ , such that

$$J = \beta \left( \frac{1}{\mu_1} - 1 \right) \quad (\text{A-15})$$

is minimized and, therefore,  $\mu_1$  is maximized. In the usual case where none of the boundary conditions involves the exhaust velocity and since  $c$  does not appear in Eq. (A-15), the quantity  $dc$  is arbitrary and Eq. (A-14) yields

$$\int_{t_0}^{t_1} \frac{\partial F}{\partial c} dt = \frac{\beta}{c^2} \int_{t_0}^{t_1} \alpha_p \left( 2L - \frac{\lambda}{\mu} \right) dt = 0 \quad (\text{A-16})$$

where the constraining relations in Eq. (1) and (2) have been incorporated into  $F$ . This condition guarantees an extremal in  $J$  with respect to  $c$ .

For the alternate optimization procedure of minimizing  $J$  with respect to initial thrust acceleration  $a_0$ , for a fixed  $c$ , it is convenient to write  $J$  in the form

$$J = c a_0 \left( \frac{1}{\mu_1} - 1 \right) \quad (\text{A-17})$$

by use of Eq. (3). If, again, the assumption is made that the boundary conditions involve neither  $a_0$  nor  $\mu_1$ , then  $da_0$  and  $d\mu_1$  are independent from the remainder of the terminal quantities and Eq. (A-9) and (A-14) yield for the minimization of  $J$  with respect to  $a_0$ , respectively

$$dJ = c \left( \frac{1}{\mu_1} - 1 \right) da_0 - \frac{c a_0}{\mu_1^2} d\mu_1 = 0 \quad (\text{A-18})$$

$$\frac{\partial F}{\partial \mu_1} \bigg|_{t_1} d\mu_1 + da_0 \int_{t_0}^{t_1} \frac{\partial F}{\partial a_0} dt = 0$$

The quantity  $d\mu(t_0)$  is zero since  $\mu_0$  is fixed at the value 1. If the quantity  $\beta$  is replaced by  $a_0 c$  in Eq. (2) and (3) and the resulting modified constraining relations are used in  $F$ , it will be found that the above system of equations yields

$$\left[ \mu(\mu L - \lambda) \right]_{t_0}^{t_1} = 0 \quad (\text{A-19})$$

as a necessary condition for an extremal in  $J$  with respect to  $a_0$  for a fixed  $c$ .

### C. Terminal Conditions

Consider the case in which the kinematic state variables are specified at both ends of the trajectory by explicit functions of time, which in the case of planetary rendezvous are simply the ephemerides of the departure and arrival planets. In cartesian coordinates the positions and velocities  $x_i, v_i$  at the terminal points may be expressed in the form

$$\left. \begin{aligned} A_i^{(0)} &= x_i(t_0) - x_i^{(0)}(t_0) = 0, \\ A_i^{(1)} &= x_i(t_1) - x_i^{(1)}(t_1) = 0 \\ A_{i+3}^{(0)} &= v_i(t_0) - v_i^{(0)}(t_0) = 0, \\ A_{i+3}^{(1)} &= v_i(t_1) - v_i^{(1)}(t_1) = 0 \end{aligned} \right\} i = 1, 2, 3 \quad (\text{A-20})$$

The superscripts 0 and 1 denote the functions corresponding to the ephemerides of the departure and arrival planets, respectively. Furthermore, suppose the flight time  $t_1 - t_0$ , is held fixed but the launch date  $t_0$  is not specified. In this case, fourteen boundary conditions have been specified. (These are Eq. A-20, fixed flight time and initial mass of unity.) The launch date and the final mass are unspecified and, consequently, there is one transversality condition available which holds at the optimum launch date extremizing  $J$ . Any parameters  $\kappa_v$ , which might exist, are assumed to not appear in the boundary conditions and are, therefore, uncoupled from the kinematic variables and need not be considered in deriving the transversality condition for optimum launch date. In cartesian coordinates the kinematic constraining equations are

$$\dot{v}_i + \frac{\partial V}{\partial x_i} - a_i = 0 = G_{i,v_i} - \dot{x}_i = 0 = G_{i+3}, \quad (\text{A-21})$$

and it follows that the Lagrange multipliers are

$$\frac{\partial F}{\partial \dot{v}_i} = \lambda_i, \quad \frac{\partial F}{\partial \dot{x}_i} = -\lambda_{i+3} = -\dot{\lambda}_i \quad (\text{A-22})$$

where the last relation follows from the Euler-Lagrange equations. From Eq. (A-20) and the constraint of constant flight time.

$$\left. \begin{aligned} dA_i^{(v)} &= dx_i(t_v) - v_i(t_v) dt_v = 0 \\ dA_{i+3}^{(v)} &= dv_i(t_v) - \dot{v}_i^{(v)}(t_v) dt_v = 0 \\ dt_1 - dt_0 &= 0 \end{aligned} \right\} v = 0, 1 \quad (\text{A-23})$$

Using these results in Eq. (A-11) and (A-14) and employing the fact that Eq. (A-7) holds, one obtains

$$(\lambda_i \dot{v}_i^{(1)} - \dot{\lambda}_i v_i)|_{t_1} - (\lambda_i \dot{v}_i^{(0)} - \dot{\lambda}_i v_i)|_{t_0} = 0 \quad (\text{A-24})$$

Since the planets travel in the same potential field as the vehicle it follows, using vector form, that the condition

$$\left[ \dot{\lambda} \cdot \dot{\mathbf{r}} + \lambda \cdot \nabla V \right]_{t_1}^{t_0} = 0 \quad (\text{A-25})$$

is the transversality condition for optimum launch date.

Although the use of cartesian coordinates in many cases allows simple derivations as above, this coordinate system sometimes tends to obscure the inherent symmetries of the problem. In Ref. 2 a spherical coordinate system has been employed and the kinematic boundary conditions have been expressed in terms of the orbital elements  $E, h, i, \omega, \Omega$ , and  $\psi$ . (See Fig. 2 and Eq. 17 through 22 of Ref. 1.) It was stated (and it may be verified using Eq. A-11 and A-14) that if the position on the terminal orbit  $\psi$ , is left unspecified but with fixed flight time (and no dependence on launch date), the transversality condition which should be satisfied for optimum rendezvous point (and least-optimum, also) was given by

$$M + N + K_1 \frac{h_\phi}{r^2} \cos \phi = 0 \quad (\text{A-26})$$

where these symbols are defined in Ref. 1. Using Eq. (17) of Ref. 1 and Eq. (8) of this report, it follows that this condition is equivalent to

$$(\dot{\lambda} \cdot \dot{\mathbf{r}} + \lambda \cdot \nabla V)|_{t_v} = 0 \quad v = 0, 1 \quad (\text{A-27})$$

Using orbital elements and including a launch date dependency, only the quantity  $\psi$  is a function of the launch and arrival dates through the ephemerides and may be expressed in the form

$$\psi(t_0) - \psi^{(0)}(t_0) = 0; \psi(t_1) - \psi^{(1)}(t_1) = 0 \quad (\text{A-28})$$

It is clear that Eq. (A-25) must still hold for optimum launch date. However, if one passes through synodic eras seeking the optimum synodic era, this is tantamount to removing the coupling between orbital positions and launch and arrival dates in Eq. (A-28); the terminal values of  $\psi$  are, in effect, unspecified and it follows that Eq. (A-25) decomposes into the two conditions in Eq. (A-27) which holds in the optimum synodic era at the optimum launch date in that synodic era. In actuality, Eq. (A-27) is never exactly satisfied at both the initial

## REVISION NO. 1

and final point, but in the year 1971 these conditions are nearly met.

If either the initial or final orbit is circular and the launch case dependency is removed, it is unnecessary to specify the transit angle  $\theta(t_1) - \theta(t_0)$ . In the spherical coordinate formulation of Ref. 1 the quantity  $r^2 \cos \phi (\partial F / \partial \theta)$  is a constant ( $K_1$ ) due to cyclic nature of the variable  $\theta$ . If  $\theta$  does not explicitly appear in the boundary conditions of Eq. (A-11) nor in  $J$ , it follows from Eq. (A-14) that  $K_1$  is zero. Consequently, if the terminal orbital position and the transit angle  $\theta(t_1) - \theta(t_0)$ , (or alternately, the longitude of the line of nodes  $\Omega$ ) are unspecified it follows from Eq. (A-26) that both Eq. (A-27) and a zero value for  $K_1$  are implied.

It should be obvious that there are any number of transversality conditions for this problem which may be developed for each unspecified variable. As a final example, consider the problem of finding the optimum launch date for any flight time when the transit angle is held fixed. One may draw curves of constant transit angle on Fig. 4. These curves depart slightly from straight lines because of the planetary eccentricities but are sloped upward and to the right, this is, increasing flight time with increasing launch date. As one travels along one of these curves there is an optimum launch date and flight time corresponding to a minimum  $J$ . Using the sole constraint that  $\theta(t_1) - \theta(t_0)$  is a constant it may be verified that the condition

$$\left[ (K_2 + \dot{\lambda} \cdot \dot{\mathbf{r}} + \lambda \cdot \nabla V) \dot{\theta}^{-1} \right]_{t_0}^{t_1} = 0 \quad (\text{A-29})$$

yields the optimum launch date.

### D. First Order Variations in $J$

For simplicity in the algebra, suppose that (1) the initial values of all the state variables are specified and (2) the boundary conditions  $A_j$  specify the final values of certain state variables and parameters leaving the remainder independent. These simplifications do not seriously affect the reasoning to follow. In this case Eq. (A-9) and (A-14) become

$$dJ = \frac{\partial J}{\partial q_i(t_1)} dq_i(t_1) + \frac{\partial J}{\partial t_1} dt_1 + \frac{\partial J}{\partial \kappa_v} d\kappa_v \quad (\text{A-30})$$

and

$$\begin{aligned} 0 &= \frac{\partial F}{\partial \dot{q}_i(t_1)} dq_i(t_1) - \dot{q}_i(t_1) \frac{\partial F}{\partial \dot{q}_i(t_1)} dt_1 \\ &+ d\kappa_v \int_{t_0}^{t_1} \frac{\partial F}{\partial \kappa_v} dt \end{aligned} \quad (\text{A-31})$$

These two linear equations in the terminal variations are generally of rank 2 affording a relationship between the terminal variations. By combining Eq. (A-30) and (A-31) one obtains expressions for the first-order variation of  $J$  with respect to the various unspecified terminal quantities.

As examples, consider the power-limited system with  $J = \mu_1$  and all the remaining state variables and parameters specified with the exception of  $c$ . It may be easily shown that the variation in  $\mu_1$  with respect to  $c$  is given by

$$d\mu_1 = \left[ \frac{\beta \cdot}{c^3 \left( L - \frac{\lambda}{\mu} \right)_{t_1}} \int_{t_0}^{t_1} \alpha_p \left( 2L - \frac{\lambda}{\mu} \right) dt \right] dc \quad (\text{A-32})$$

In a similar fashion with  $J$  given by Eq. (A-17), it may be shown that the variation in  $J$  with respect to  $a_0$  is given by

$$dJ = c \left[ \frac{(\lambda - \mu L)_{t_0}}{\mu_1 (\lambda - \mu L)_{t_1}} - 1 \right] da_0 \quad (\text{A-33})$$

As another type of example, suppose  $J$  is to be extremized with respect to all the unspecified terminal quantities, in which case,  $dJ = 0$  in Eq. (A-30). It follows at  $t_1$

$$\frac{\partial J}{\partial q_i} = \rho \frac{\partial F}{\partial \dot{q}_i}; \quad \frac{\partial J}{\partial t_1} = -\rho \dot{q}_i \frac{\partial F}{\partial \dot{q}_i}; \quad \frac{\partial J}{\partial \kappa_v} = \rho \int_{t_0}^{t_1} \frac{\partial F}{\partial \kappa_v} dt \quad (\text{A-34})$$

where  $\rho$  is an arbitrary proportionality constant which, for convenience, may be set to equal 1 by the appropriate scaling of the Lagrange multipliers defined in Eq. (A-2). Let perturbations or variations of the state variables from the optimum values occur at some point on the trajectory earlier than  $t_1$  and denote these variations by  $\delta q_i$ . Then by Eq. (A-14) and (A-34), the variation in  $J$  due to these perturbations is given by

$$\delta J = \frac{\partial F}{\partial \dot{q}_i(t)} \delta q_i(t) \quad (\text{A-35})$$

where it is assumed that the original boundary conditions are still satisfied. Equation (A-35) is a valuable expression in guidance considerations since it affords a means of estimating the degradation in vehicle performance due to errors of execution in the controls of the system and in observations of the state of the system.